GENE Open

Genes and Immunity (2010) 11, 1–10
© 2010 Macmillan Publishers Limited All rights reserved 1466-4879/10 $32.00
www.nature.com/gene

ORIGINAL ARTICLE

A functional SNP in the regulatory region of the decay-accelerating factor gene associates with extraocular muscle pareses in myasthenia gravis

JM Heckmann[1], H Uwimpuhwe[1,2], R Ballo[1,2], M Kaur[3], VB Bajic[3,4] and S Prince[2]

[1]Neurology Research Group, Department of Medicine, University of Cape Town, Cape Town, South Africa; [2]Department of Human Biology, University of Cape Town, Cape Town, South Africa; [3]South African National Bioinformatics Institute, University of the Western Cape, Cape Town, South Africa and [4]Computational Bioscience Research Center, King Abdullah University of Science and Technology, Thuwal, Kingdom of Saudi Arabia

Complement activation in myasthenia gravis (MG) may damage muscle endplate and complement regulatory proteins such as decay-accelerating factor (DAF) or CD55 may be protective. We hypothesize that the increased prevalence of severe extraocular muscle (EOM) dysfunction among African MG subjects reported earlier may result from altered DAF expression. To test this hypothesis, we screened the DAF gene sequences relevant to the classical complement pathway and found an association between myasthenics with EOM paresis and the DAF regulatory region c.-198C>G SNP (odds ratio=8.6; P=0.0003). This single nucleotide polymorphism (SNP) results in a twofold activation of a DAF 5′-flanking region luciferase reporter transfected into three different cell lines. Direct matching of the surrounding SNP sequence within the DAF regulatory region with the known transcription factor-binding sites suggests a loss of an Sp1-binding site. This was supported by the observation that the c.-198C>G SNP did not show the normal lipopolysaccharide-induced DAF transcriptional upregulation in lymphoblasts from four patients. Our findings suggest that at critical periods during autoimmune MG, this SNP may result in inadequate DAF upregulation with consequent complement-mediated EOM damage. Susceptible individuals may benefit from anti-complement therapy in addition to immunosuppression.
Genes and Immunity (2010) **11,** 1–10; doi:10.1038/gene.2009.61; published online 13 August 2009

Keywords: *myasthenia gravis; complement; extraocular muscles; decay-accelerating factor; CD55; regulatory single nucleotide polymorphism*

Introduction

Antibody-mediated damage at the neuromuscular junction in myasthenia gravis (MG) is largely because of concomitant activation of the classical complement pathway.[1,2] Although IgG1–acetylcholine receptor (AChR) complexes can modulate AChRs by cross-linking and accelerating degradation as well as functionally blocking AChRs, it is the activation of complement through successive stimulation of C3 and C5 convertase that ultimately results in a membrane attack complex with lysis of the post-synaptic muscle endplate.[3,4] There is a body of data implicating complement in the pathophysiology of MG; complement deposition has been observed at the muscle endplate of human subjects with MG and in experimental allergic MG (EAMG).[1,3,5] Animal models became resistant to the induction of EAMG when circulating complement was either depleted by cobra venom toxin or functionally inhibited by the administration of a monoclonal C5 antibody or soluble C1 receptor.[6–8] Rodent models either deficient in C4, critical for the generation of C3 convertase, or C6, an important constituent of the membrane attack complex, were more resistant to EAMG induction[9,10] and showed less endplate damage than control animals.[9] Complement-mediated damage at the muscle endplate has been shown to result in the loss of AChRs, alter the architecture of endplate folds and likely reduce Na^+ channel density in these folds, all of which affects neuromuscular transmission.[11]

Innate complement control mechanisms include complement regulatory proteins expressed on all serum-exposed cells, each of which intervenes at key points in the cascade, thereby protecting cell membranes against autologous complement damage. One of these is decay-accelerating factor (DAF) or CD55, and its main function is to bind and inactivate pre-formed C3/C5 convertase complexes.[12,13] Both DAF and, another complement regulator, CD59, appear to be concentrated at neuromuscular junctions and both can be upregulated by muscle cells.[14] Of the two, DAF appears to be more crucial in the protection of muscle against EAMG-associated complement injury,[15] although this finding may be mouse strain-specific.[16] *Daf1*-deficient animals compared with wild-type (WT) littermates were

Correspondence: Associate Professor JM Heckmann, Division of Neurology, University of Cape Town, Room E8-74, Groote Schuur Hospital, Observatory, Cape Town 7925, South Africa.
E-mail: jeanine.heckmann@uct.ac.za
Received 10 November 2008; revised 25 June 2009; accepted 9 July 2009; published online 13 August 2009

more susceptible to EAMG induction and suffered more severe complement-mediated muscle damage.[2,15]

From clinical observations, a larger proportion of South African (SA) subjects with African genetic ancestry (either indigenous Black African (Black) or mixed ancestry (M/A)) were noted to develop severe myasthenic extraocular muscle (EOM) dysfunction (including levator palpebrae muscles); almost half of these patients only developed this ocular phenotype while receiving standard immunosuppressive therapy, with the remaining MG signs responding appropriately to therapy.[17] DAF provides substantial complement protection for eye tissues,[18] and as the expression of DAF in the EOMs of mice is substantially lower than other skeletal muscle allotypes,[14,19] we reasoned that MG patients developing severe EOM damage may have lower background or inducible DAF expression.

The *DAF* gene maps to chromosome 1q32 and consists of 14 exons that encode a 70-kDa protein.[20,21] The functional sites are organized into four N-terminal complement control protein (CCP) domains separated from a C-terminal glycophosphatidylinositol (GPI) membrane anchor by the serine, threonine and proline stalk.[22] Site-directed mutagenesis determined that the CCP 2 and 3 regions are critical for the classical pathway C3 convertase regulatory activity,[23] and are encoded by exons 3, 4 and 5.[20] A number of DAF isoforms have been characterized. The two major splice variants are membrane-bound DAF (gDAF) and soluble DAF (sDAF) found in plasma and body fluids.[21,24] Isoform switching from sDAF to gDAF occurs when exon 10 is spliced out.[21] The last exon encodes the GPI anchor, which is attached and guided by a critical signal, the C-terminal serine 319, to the cell membrane for insertion.[25]

The 'minimal *DAF* promoter' or the 5′-flanking region has several regulatory regions that show functional variation in different cell lines, suggesting tissue specificity in transcriptional regulation.[26–28] Furthermore, there is increasing evidence of single nucleotide polymorphisms (SNPs) in regulatory elements influencing variation in gene expression and susceptibility to complex diseases.[29] On the basis of these observations, we hypothesize that DAF expression may be lower than normal or not properly upregulated during 'inflammatory stress,' resulting in inadequate complement protection in the EOMs of a subgroup of individuals with MG. We screened the *DAF* gene sequence of subjects with the severe EOM phenotype focusing initially on exons encoding the regions important in the regulation of the classical complement pathway, and second on the *DAF* gene regulatory sequence, which would influence gene expression. We found evidence that an alteration of the *DAF* regulatory sequence, the c.-198C > G SNP, associates with a severe EOM outcome in MG and suggest (a) the loss of a Sp1-binding site and (b) that altered upregulation of DAF expression to a lipopolysaccharide (LPS)-like stimulus during the MG disease course may influence MG morbidity.

Results

Clinical data

The EOM outcome to standard MG therapy was based on data from symptom onset to analysis over a median period of 6 years (interquartile range (IQR): 3, 13.5); the observational period for Black (median: 7.0 years; IQR: 2.5, 11.75) and White patients (median: 5.0 years; IQR: 2.5, 7.0) ($P = 0.104$) was similar, although M/A patients had been followed for longer period (median: 8.5 years; IQR: 3.55, 17.75). Genotyping was carried out in 139 MG patients and 167 controls (Table 1). See additional material (Supplementary Table S1) for the distribution of MG subtypes studied. At diagnosis, most MG patients had paresis of at least one EOM that, in the majority, subsequently resolved on immunosuppressive therapy.[17] However, during the MG disease course and on immunotherapy, patients of African ancestry were more likely to develop dysfunction of at least one EOM (26.5%; 95% CI: 18.6, 35.7) compared with Whites (15.2%; 95% CI: 5.8, 30.4), with an even greater racial disproportion when those with pareses of five or more EOMs are categorized (20.6 vs 9.1%, respectively) (Table 1). Of the 30 subjects with more than one EOM paresis, only 1 had ocular MG (complete ophthalmoplegia previously described[17]), 3 were seronegative (and MuSK negative) and 1 had concomitant thyroid disease (excluded from analysis). Those with complete ophthalmoplegia also had bilateral ptosis at rest.[17] Supplementary Figure 1 shows the distribution of EOM dysfunction in those with African ancestry compared with those without; all the subjects with pareses of $\geqslant 5$ EOMs had at least unilateral ptosis at rest and those with pareses of $\geqslant 9$ EOMs also had bilateral ptosis.

DAF sequencing

Exons 3, 4 and 5 were sequenced in 49, 56 and 44 individuals with MG, respectively, and the results showed no differences to the published sequences (http://www.ncbi.nlm.nih.gov/entrez). Sequencing of the *DAF* upstream regulatory region[26] detected two variants (rs28371585 and rs28371586) with the SA subpopulation control frequencies similar to those of previously genotyped racially matched controls; SA White controls were similar to European controls, and SA Black and M/A controls were similar to African-American controls (Table 1 and Supplementary Table S2; http://www.ncbi.nlm.nih.gov/SNP). SNP rs28371585 (c.-244_–243insA) was found to be prevalent among controls with African genetic ancestry (37%) and showed a trend toward reduced prevalence among MG subjects (26%; odds ratio = 0.61; $P = 0.085$) (Supplementary Table S2).

The sequence of the cDNA spanning exons 7–9/14 gDAF was normal in 10 MG subjects, including individuals with severe MG-associated ophthalmoplegia and refractory MG.

DAF regulatory region SNP as susceptibility allele for the development of EOM paresis in MG

The allelic frequencies and genotypes of the *DAF* c.-198C > G SNP (rs28371586) in three sub-populations of myasthenic subjects are shown in Table 1. This SNP in the upstream regulatory region of *DAF* showed no significant association with MG subjects overall, but was significantly more frequent among those developing EOM paresis associated with MG. Of the 11 patients presenting with complete ophthalmoplegia at the time of MG diagnosis, 4 responded partially to immunotherapy or not at all, and 2 of these had the c.-198C > G SNP. Five patients developed complete ophthalmoplegia only after

Table 1 Association of rs28371586 (c.-198C>G) with treatment-resistant EOM involvement in South African MG sub-populations

Subjects			*G allele*			*Genotype*		*CG+GG/CC*	
	Phenotype	N *(%)*	*Frequency*	*OR (95% CI)*	P-*value*	*CC*	*CG/GG*	*OR (95% CI)*	P-*value*
Black	EOM-N	21 (70)	0			1.0	0		
	EOM ⩾1	9 (30)	0.222	**12.9** (2.1–108.7)	**0.006**	0.555	0.444	**18.4** (2.7–127.0)	**0.004**
	EOM ⩾5	6 (20)	0.250	**14.6** (2.0–138.6)	**0.009**	0.500	0.500	**23.0** (2.7–194.8)	**0.008**
	C	48	0.021			0.958	0.042		
M/A	EOM-N	53 (74)	0.009			0.981	0.019		
	EOM ⩾1	18 (25)	0.111	**6.2** (1.3–29.1)	**0.022**	0.833	0.167	4.0 (0.8–19.7)	0.12
	EOM ⩾5	15 (21)	0.067	2.9 (0.4–17.2)	0.27	0.867	0.133	3.1 (0.5–18.5)	0.28
	C	84	0.024			0.952	0.048		
Afr-ancest	EOM-N	75 (74)	0.006			0.987	0.013		
	EOM ⩾1	27 (26)	0.148	**8.6** (2.8–26.1)	**0.0003**	0.740	0.259	**7.4** (2.2–24.1)	**0.002**
	EOM ⩾5	21 (21)	0.119	**5.8** (1.5–20.7)	**0.011**	0.762	0.238	**6.6** (1.8–24.0)	**0.009**
	C	132	0.023				0.045		
White[a]	EOM-N	28 (85)	0			1	0		
	EOM ⩾1	5 (15)	0			1	0		
	EOM ⩾5	3 (9)	0			1	0		
	C	35	0			1	0		
SNP-NCBI (ss32475790)									
Af-Amer		23	0.022			0.978	0.043		
European		23	0			1	0		

Abbreviations: Af-Amer, African American; Afr-ancest, African ancestry, i.e., indigenous Black Africans and those with African admixture (M/A); C, racially matched controls; CI, 95% confidence interval; EOM, extraocular muscles; EOM-N, normal eye movements; M/A, mixed ancestry; MG, myasthenia gravis; OR, odds ratio.
Bold values indicate the significant ORs.
[a]One subject with thyroid eye disease was excluded from the analysis.
EOM ⩾1 refers to at least 1 EOM paresed and unresponsive to therapy for several months; EOM ⩾5 refers to paresis of at least 5 of 12 EOMs. Odds ratio were determined relative to the normal controls and the exact *P*-values are two-tailed.

MG was diagnosed and immunotherapy initiated, and three had the c.-198C>G SNP. Of all the MG subjects followed up, nine had at least one G allele, of whom only one had full EOM movement. The highest likelihood of developing severe ophthalmoplegia associated with MG appears to be in a Black individual with either the G/C or GG genotype.

The DAF c.-198C>G SNP is regulatory

The c.-198C>G SNP created through site-directed mutagenesis in a human *DAF* 5′-regulatory region, and hereafter referred to as the 'Mut *DAF* promoter,' influenced basal activity of the *DAF* regulatory region. In COS-7, HT1080 and C2C12 muscle cells, we showed a 2- to 2.5-fold increase in luciferase activity driven by the Mut *DAF* promoter compared with the WT 5′-regulatory sequence (Figures 1a and b). Although the C2C12 muscle cells showed evidence of myoblast differentiation after 2 (fusiform elongation and 85% confluence) to 4 days (multinucleation) in differentiation medium, allowing the cells to differentiate for 10 days showed no difference in relative luciferase activity between WT and Mut *DAF* vectors (Figure 1b). Figure 1c shows the absolute quantified mRNA expression of g*DAF* from three lymphoblastoid cell lines from patients with the c.-198C>G SNP in the *DAF* 5′-regulatory region. Furthermore, basal *DAF* expression was higher in two cell lines with the Mut *DAF* promoter compared with the WT, mimicking the results of the *in-vitro* transfection experiments.

Loss of a transcription factor-binding site

The transcription factor-binding site (TFBS) analysis showed that the WT *DAF* 5′-flanking sequence contains an Sp1-binding site that is lost in the Mut *DAF* 5′-flanking sequence, whereas the Mut sequence showed gain of a nuclear factor-κB (NF-κB) TFBS. To investigate the functional importance of the loss of an Sp1 TFBS at c.-198C>G of the *DAF* regulatory region, co-transfection experiments were carried out in HT1080 cells with an Sp1 expression vector (pCMV-Sp1) or an empty vector (pCMV) in addition to the Mut or WT *DAF* promoter luciferase vector. Sp1 had a similar effect on both the WT and the Mut *DAF* promoters (Figure 2).

The DAF 5′-flanking region c.-198C>G SNP influences LPS-induced DAF upregulation

The transcription factor Sp1 induces *DAF* expression in response to LPS treatment. The expected inducible response of the WT *DAF* regulatory region with an increase in gDAF mRNA and protein expression in response to LPS treatment compared with cells treated with vehicle alone is shown in Figures 3a–c. However, lymphoblasts from four MG patients with the c.-198C>G SNP showed a reduction in gDAF mRNA and protein expression upon LPS stimulation, presumably because of the loss of the Sp1 TFBS at c.198 of the *DAF* regulatory region.

Quantification of gDAF protein expression by western blotting (Figures 3b and c) shows the WT gDAF expression to be approximately 2.4-fold upregulated to

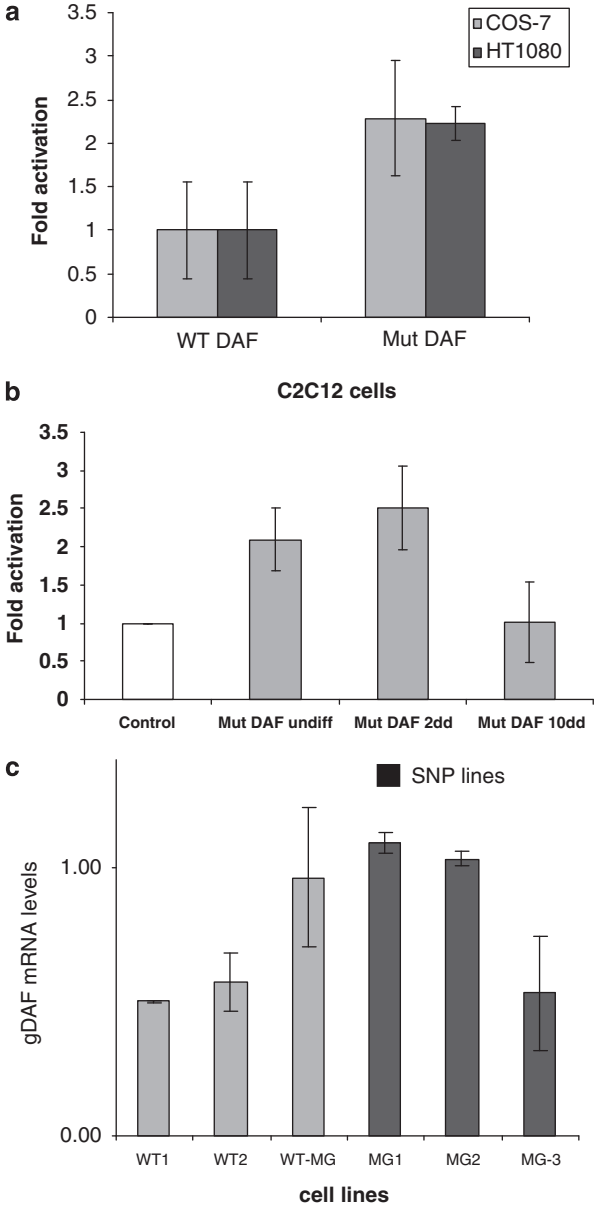

Figure 1 The c.-198C>G (mutant) DAF SNP is regulatory. (**a**) Transfection of the mutant *DAF* regulatory construct activates *DAF* promoter activity (as measured by luciferase assay) compared with transfection with WT promoter construct in COS-7 and HT1080 cells (normalized to 1); the plasmid pRL-TK (50 ng) containing the thymidine kinase promoter driving the expression of a *Renilla* reporter was used as an internal control for transfection efficiency and firefly luciferase activity was normalized to *Renilla* luciferase activity. Results representative of two independent experiments carried out in duplicate. (**b**) Luciferase assay in C2C12 muscle cells transfected with the mutant *DAF* promoter compared with WT controls (normalized to 1) shows activation at 0–2 days of differentiation. Mean data (±s.d.) of duplicate experiments. Undiff, undifferentiated; 2dd, 2 days in differentiation; and 10dd, 10 days in differentiation medium. (**c**) Quantitative RT-PCR of gDAF mRNA extracted from lymphoblastoid cell lines from three patients with the c.-198C>G (MG1 to MG3), one MG patient without the SNP (WT-MG) and two controls (WT1 and WT2). Absolute mRNA expression levels (normalized to GUS1B) are extrapolated from a standard curve. Data (mean±s.d.) from two independent experiments carried out in duplicate and expressed as fold change over non-LPS controls.

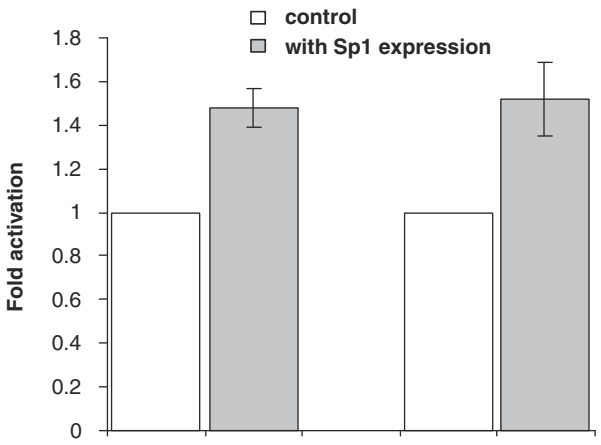

Figure 2 Co-transfection of the *DAF* promoter construct and the Sp1 vector in HT1080 cells does not alter basal activity. The average fold change of luciferase activity from cells co-transfected with empty vector (pCMV) as control relative to those transfected with Sp1 transcription factor (pCMV-Sp1), in addition to either WT or mut *DAF* promoter, is similar. Mean data (±s.d.) of duplicate experiments.

LPS treatment, whereas the SNP cell line is approximately 2.4-fold downregulated in response to LPS treatment.

Discussion

Much data exist implicating complement as a major effector in neuromuscular junction damage in MG.[1–12,14–16] Knockout experiments have shown that complement regulators such as DAF, at least in the EAMG model, influences the severity of damage by complement-fixing antibodies at the muscle endplate.[2,15,16] Although basal complement regulatory protein (CRP) mRNA transcripts were lower in mouse EOMs compared with their diaphragm muscles, the induction of EAMG resulted in a further reduction of EOM CRP expression and particularly of DAF.[14] These and other observations led to the 'complement hypothesis,' suggesting that a relative deficiency of complement regulation in extraocular muscles may increase their susceptibility to myasthenic induction.[14,30] This study represents the first supportive evidence in humans; our data show that DAF is linked to the development of a treatment-resistant EOM phenotype that develops in a subgroup of MG patients; myasthenic subjects with the c.-198C>G SNP in the regulatory region of the *DAF* gene have a significantly higher risk of developing EOM pareses. The c.-198C>G SNP influences *DAF* regulation and specifically the ability to upregulate DAF expression in response to bacterial products such as LPS, which we propose, may influence the degree of complement-mediated endplate damage at critical periods during the patient's myasthenic disease course.

Transfection of the Mut *DAF* 5′-flanking region (containing a mutation mimicking the SNP) cloned into a luciferase reporter vector shows the SNP to be functional and capable of driving luciferase expression in three different cell lines under basal conditions. Similarly, absolute DAF mRNA expression in EBV-transformed lymphoblasts from two individuals with

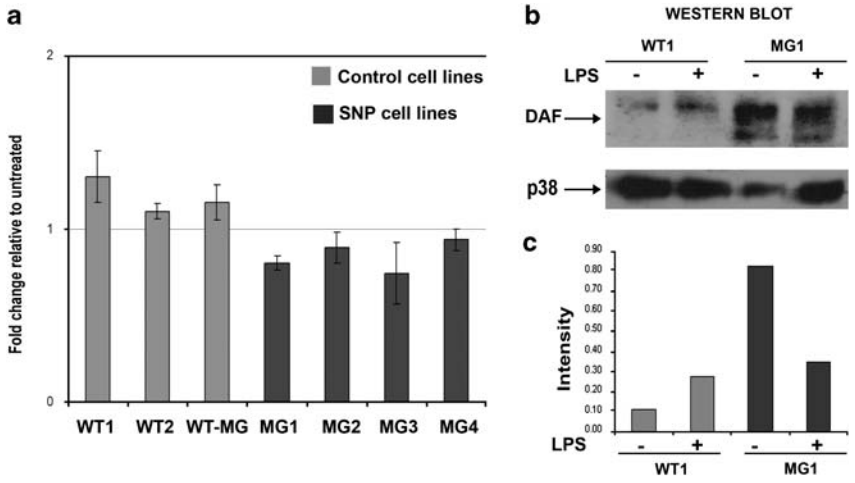

Figure 3 Effect of LPS treatment on gDAF RNA and protein expression in lymphoblasts. (**a**) Total RNA was extracted from lymphoblast cell lines from three controls (WT1 and WT2 and one MG patient without the SNP, WT-MG) and four MG patients with the c.-198C>G SNP (MG1 to MG4), with and without LPS stimulation (10 μg/ml) for 6 h. Relative expression (normalized to GUS1B) by qRT-PCR is shown expressed as fold change over non-LPS control for each cell line (normalized to 1). Data (mean ± s.d.) from triplicate experiments. (**b**) Western blot analysis of DAF protein levels in control (WT1) and MG patient (MG1) derived cell lines. The cells were treated with 10 μg ml^{-1} of LPS for 6 h. Protein was extracted under non-reducing conditions and quantified using BCA standard curve method (Materials and methods). For each sample, 30 μg of protein was loaded on an SDS-PAGE gel and p38 was used as a loading control to ensure equal loading of protein. DAF protein levels increased in control cell line but decreased in the MG patient cell line on treatment with LPS. (**c**) The bar graph represents quantitative DAF protein results by showing densitometry readings from the autoradiograph of DAF protein levels normalized to p38 protein levels. For the control cell line, DAF protein levels showed an increase of approximately two-folds as a result of LPS treatment. On the contrary, the MG SNP cell line showed a decrease of approximately two-fold when treated with LPS.

the c.-198C>G SNP was also unexpectedly higher compared with that in controls. Direct matching of known binding sites to the surrounding of the SNP shows the Mut SNP sequence to result in a potential gain of an NF-κB-binding site and a loss of an Sp1-binding site present in the WT sequence. In mouse studies, the regulatory region of *Daf1* was shown to have several Sp1 transcription binding sites that are critical in the constitutive and LPS-inducible expression of Daf in several tissues.[28] Two of three Sp1 sites in the *Daf1* promoter (+1 to −619) were critical for the basal *Daf1* promoter activity in several cell lines, whereas the remaining non-critical Sp1 site that equates with the Sp1 site lost in the human c.-198C>G SNP did not influence basal transcription.[28] Interestingly, deletion of the latter Sp1 site in mice also resulted in the activation of *Daf1*-driven luciferase activity in mouse B cells.[28]

Several studies have shown that bacterial LPS, a major component of Gram-negative bacterial cell walls, upregulates DAF expression (Cauvi *et al*.[28]). LPS-induced upregulation of the regulatory activity and the expression of *Daf1* were shown in both murine lymphocyte and macrophage cell lines but not in fibroblasts, suggesting tissue specificity of LPS-induced DAF upregulation.[28] The LPS-induced DAF upregulation in these mouse cells were predominantly dependent on the two Sp1 sites most proximal to the transcription start site,[28] excluding the herein described putative Sp1 site lost with the SNP. Although our studies in human control lymphoblasts showed the expected LPS treatment-induced DAF expression, the lymphoblast containing the c.-198C>G SNP showed a reduction in gDAF mRNA and protein levels after LPS stimulation. Thus, the loss of the Sp1 site at c.-198C>G in the *DAF* 5′-flanking region results in a downregulatory response to LPS stimulation in human lymphoblasts. Although we cannot be certain of the effect that the c.-198C>G SNP may have in human extraocular muscles, we do know that the SNP showed similar responses in transfection experiments in mouse muscle cell lines to that observed in human lymphoblasts under basal conditions.

Constitutive DAF expression is modulated by several cytokines (interleukin (IL)-1, IL-6, tumor necrosis factor-α (TNF-α), transforming growth factor (TGF)-β1 and interferon (IFN)-γ), prostaglandins and other tissue-specific factors, although primary regulation is believed to be at transcriptional level.[27,28] The transcription factor Sp1 is present in the nuclei of all cells with the potential of transcriptional activation upon binding to the DNA Sp1-binding sites.[31] Studies have shown that cooperative complex formation between several closely positioned Sp1 sites are required for full gene expression.[32,33] Although proximal (to the transcription start site) Sp1-binding sites are critical for basal transcription, such as was seen in the *Daf1* promoter,[28] the additional cooperation of more distal Sp1 sites (such as that lost in our Mut *DAF* with the SNP) may be necessary for an enhanced or higher level of expression.[33,34] This does not explain why the Mut *DAF* showed higher basal expression compared with WT *DAF*, but it does offer an explanation for the inability of the Mut *DAF* to upregulate transcription in response to a known induction signal such as LPS.

There is increasing evidence of SNPs in the proximal region upstream of transcription start sites to act as specific functional *cis*-regulatory variants.[29,34,35] The human *DAF* 5′-flanking sequence has been shown to harbor several regulatory regions including an enhancer region that is highly conserved and that encompasses the Mut *DAF* SNP site (−206/−77 and −206/−34).[26–28] It is possible that the regulatory SNP at c.-198C>G in humans results in increased *DAF* basal promoter activity either due to functional loss of an inhibitory element or

due to the gain of an enhancer. Computational analysis of the Mut 5′-flanking region suggested the gain of a NF-κB-binding site. The NF-κB/Rel family of transcription factors is involved in a wide range of inflammatory signaling accomplished either by functional interaction with other transcription factors or by variation in the composition of the NF-κB dimers that translocate to the nucleus and bind DNA.[36] Subtle differences in NF-κB-binding sites may favor certain dimer combinations with varied functional transcriptional consequences.[36] We plan to study the effects of the putative gain of a NF-κB TFBS in the future.

DAF has other functions apart from complement regulation; antigen-primed T cells deficient of the *Daf1* gene showed enhanced responsiveness and greater pro-inflammatory cytokine production influencing inflammatory-associated injury in a tissue microenvironment.[37,38] Furthermore, the augmented T-cell responsiveness to activation stimuli in *Daf1* knockout mice studies persisted for weeks.[38] A recent study in EAMG suggests that inhibiting complement at the C5 activation step, a DAF target, may also influence the humoral response with altered antibody profiles.[39] Thus, the effect of the c.-198C>G SNP on DAF regulation during the autoimmune response in a compartment such as the EOM may occur at both complement and T-cell modulation levels. Reviewing the clinical data on our cases developing the severe ocular phenotype,[17] it was evident that persistent non-fatigable EOM pareses often only developed months into the MG disease process, suggesting that it was dependent on a critical factor(s) additional to the autoantibody-mediated immune response.

In humans, dysfunctional DAF is implicated in the acquired condition of paroxysmal nocturnal hemoglobinuria, in which erythrocytes develop an increased sensitivity to complement lysis.[40,41] Moreover, a few rare individuals have been identified as having the Cromer phenotype of blood group antigens (INAB), in whom polymorphisms within the *DAF* gene result in low or no DAF expression.[42] These individuals are otherwise well, although some have developed inflammatory bowel disease.[43] Although *Daf* deficiency in knockout mouse models resulted in more severe generalized MG, we have not been able to find any other abnormalities in the *DAF* gene to explain the pathogenesis in all the patients in our cohort developing severe ophthalmoplegia; the coding regions for CCP 2 and 3 were screened for polymorphisms in a range of myasthenic individuals, and the cDNA region encoding the stalk and GPI-attachment region for gDAF was screened in a few highly selected refractory MG subjects, suggesting an intact signal for membrane targeting of gDAF. Another issue that we have been unable to address is the tissue specificity of DAF regulation or the possible context specificity of the regulatory SNP in EOM tissue. Peripheral B lymphocytes is not ideal for studying LPS-induced DAF expression,[44] and our hypothesis is based on DAF expression in human EOMs that are unobtainable, specifically when the tissue destructive phase is active. Interestingly, in a systemic autoimmune disease mouse model, the protective effect of *Daf1* on an autoimmune genetic background influenced tissue-specific skin inflammation.[45] We suggest a similar tissue-specific effect of DAF, which in certain conditions such as that mimicked by LPS influences the EOM outcome in a subgroup of patients with active MG.

In conclusion, we present evidence for the first time that the complement-regulating protein DAF may be critical for protecting the integrity of EOMs under certain inflammatory conditions mimicked by bacterial LPS in the setting of MG. MG subjects with the c.-198C>G SNP in the *DAF* regulatory region have an added risk of developing ophthalmoparesis, probably because of insufficient upregulation of DAF expression at critical periods of the autoimmune process rendering their EOMs vulnerable to complement-mediated damage. Complement inhibition therapy with a blocking anti-C5 antibody has shown promise in a rodent model of EAMG.[46] A candidate therapy in our patients would be eculizumab, a monoclonal antibody to C5 that has shown efficacy in paroxysmal nocturnal hemoglobinuria.[47] Potentially, susceptible MG patients would be screened for the polymorphism and as soon as treatment-resistant ophthalmoparesis ensues, appropriate additional anti-complement therapy may be initiated. Intravenous immunoglobulin also reduces complement factors C3a and C5a,[48] and, although expensive, would be a reasonable intervention to attempt early on in susceptible individuals in an effort to reduce the significant morbidity associated with ophthalmoplegic complications.

Materials and methods

Patients

Peripheral blood was collected from 139 unrelated MG patients, diagnosed as previously described.[17] Observational data were collected at each clinic visit. Owing to a high proportion of EOM dysfunction noted in our patients, a grading system for scoring limitation of EOMs was introduced to quantify the number of EOMs showing limitation of movement;[17] Supplementary Figure S1 denotes the number of individuals with EOM paresis at rest (excluding those whose EOM show fatigability). EOM paresis scoring was carried out before and independent of genotyping.

In addition, 167 healthy controls (hospital or university employees) were recruited for the study and informed written consent was obtained from patients and controls for blood sampling and DNA analysis. The subjects categorized themselves according to SA census racial categories as White (European ancestry), M/A or Black (indigenous African). The M/A sub-population is composed of an admixture of Khoi San, Indian, Indonesian, Black African and European ancestors. Permission for the study was granted by the UCT Research Ethics committee.

DNA was extracted using the Genomic DNA purification Kit (PUREGENE DNA Purification System, Gentra Systems, Minneapolis, MN, USA). cDNA was prepared from the total mRNA of selected patients and controls using the PAXgene tubes and Blood RNA extraction Kit (PreAnalytiX, Qiagen, Darmstadt, Germany).

PCR

Exons 3, 4 and 5 were amplified from genomic DNA using intronic primers spanning those exons. The gDAF isoform was amplified from cDNA templates using a sense primer upstream of the serine 319 site and an

Table 2 Regions amplified in the *DAF* gene

Oligonucleotides	*Sequence*	*Annealing temperature (°C)*	*Number of bases*
Promoter sense	5′-ACACCCCGTTTGTTTTACG-3′	60	20
Promoter antisense	5′-GCACAACAGCACCAGCAG-3′	60	18
Exon 3 sense	5′-TTGCTGCTTTTGTTAATACTTTTAGG-3′	60–56	26
Exon 3 antisense	5′-TATTTCCCCCAAACACCAGA-3′	60–56	20
Exon 4 sense	5′-CATAGTTACCTTCTTTGTGTGTATGC-3′	63	26
Exon 4 antisense	5′-GTCCTAATTTGTTTTCTCATTTCC-3′	63	24
Exon 5 sense	5′-CCTGGAGAATTTGAGGAAAGT-3′	63	21
Exon 5 antisense	5′-GCCTCACAATCTGAGTGCTT-3′	63	20
cDNA exon 7–9/14 sense	5′-GGATTCACCATGATTGGAGAGC-3′	53–50	22
cDNA exon 7–9/14 antisense	5′-TGTGCCCAGATAGAAGAC-3′	53–50	19

Abbreviation: DAF, decay-accelerating factor.

antisense primer that spanned the exon 9/14 boundary, thereby excluding exons 10–13 in the PCR product. All oligonucleotides were designed from sequences listed in the human genome database (http://www.ncbi.nlm.nih.gov/entrez) (Table 2). Generally, PCR of exons 3, 4 and 5 was carried out in a volume of 25 μl using 100 ng of genomic DNA and a final concentration of 10 pmol of each primer, 200 μM dNTPs, 1 × BioTaq reaction buffer, 1.5 mM $MgCl_2$ and 1 U BioTaq DNA polymerase (Bioline Ltd, London, UK). The amplification conditions for exons 4 and 5 were as follows: 94 °C (5 min) followed by 25 cycles at 94 °C (30 s), 63 °C (30 s), 72 °C (30 s) and a final extension at 72 °C (7 min) in a GeneAmp PCR System 2700 (Applied Biosystems, Foster City, CA, USA). Touchdown PCR was used for exon 3 (60–56 °C) and exons 7–9/14 (gDAF) (53–50 °C). The high GC content of the DAF regulatory region was optimally amplified using 1 × FailSafe buffer (Epicentre Biotechnologies, Madison, WI, USA) at 60 °C annealing temperature.

Sequencing
Cycle sequencing reactions were carried out using the BigDye Terminator Cycle Version 3.1 Sequencing Kit according to the manufacturer's instructions (Applied Biosystems) and analyzed on an ABI Prism 3100 automated sequencer (Applied Biosystems) using the ABI DNA Sequencing Analysis Software version 3.7. The sequences were analyzed for any changes from the known sequence by using the Clustal Alignment tool in BioEdit version 7.0. (Ibis Biosciences, Carlsbad, CA, USA).

Quantitative real-time PCR
RNA was extracted from EBV-transformed B-cell lines using the RNeasy Plus Mini kit (Qiagen). Reverse transcription of RNA (1 μg) was carried out using the ImProm-II kit from Promega (Madison, WI, USA) as recommended by the manufacturer. Using 1 μl of cDNA, PCR was conducted using SensiMix *Lite* Kit (Quantace, London, UK) with minor modification to the manufacturer's protocol. Real-time PCR was carried out on a LightCycler 2 (Roche, Mannheim, Germany) and analyzed using the LightCycler software version 3.5. The cycling conditions were as follows: 15 min at 95 °C for the initial activation of the enzyme, followed by 35 cycles of denaturation (5 s at 95 °C), annealing (3 s at 57 °C) and extension (5 s at 72 °C). Melting curve analysis was carried out to ensure product specificity by subjecting the samples to 95 °C, followed by cooling to 65 °C with a ramp rate of 0.1 °C/s. Each DNA sample was quantified in duplicate and a negative control was run with every assay to assess overall specificity. Data was analyzed using the $2^{-\Delta\Delta C_T}$ method.[49]

Relative gDAF mRNA expression levels were normalized to the housekeeping gene, Glucuronidase B (GUS1B), for each reaction. GUS1B was amplified separately in 10 μl reaction volumes, as described for DAF, using the appropriate primer set and at annealing temperature of 55 °C. The melting curve analysis was the same as for DAF.

Relative and absolute quantification methods were used to analyze the basal DAF mRNA expression levels. For LPS-induced expression, triplicate experiments were carried out for each cell line and expressed as fold change over non-LPS-treated controls. The relative quantification method was used to evaluate the quantitative real-time PCR data.[50,51] Briefly, this was accomplished by comparing the threshold cycle (C_t) values of gDAF with that of the housekeeping gene to account for differences in quality and quantity between individual samples. Standard curves were generated using serial dilutions from 10^3 to 10^7 concentrations of the external reference sample and were used for amplification efficiency correction. The dilutions were run in triplicates. An external reference cDNA sample chosen from the healthy controls was always included in each run to account for variations between runs.

The external standard reference sample enabled us to compare different PCR runs and for efficiency correction. Crossing point cycle numbers were plotted against the logarithm of the concentration of each sample to generate the standard curve. The slopes (S) were then obtained and the amplification efficiencies (E) were calculated using the formula $E = 10^{(-1/S)} - 1$. Calculated efficiency was 88.4% for gDAF and 86.9% for GUS1B.

Cell culture
COS-7 monkey kidney epithelial, HT1080 human fibrosarcoma (ATCC CCL-120) and the C2C12 mouse myoblast cell line were maintained in DMEM (Dulbecco's modified Eagle's medium), supplemented with 10% of fetal calf serum (Gibco, St Louis, MO, USA) and 1% penicillin–streptomycin (P/S) at 37 °C (95% air, 5% CO_2, 65% humidity). C2C12 cells were allowed to differentiate by switching growth medium to differentiating medium (DMEM supplemented with 2% horse serum (HS) and

1% P/S). C2C12 cells were harvested at different differentiating time points.

To establish the human lymphoblastoid cell lines by EBV transformation, 10 ml heparinized blood was obtained from four MG patients with c.-198C>G SNP and three control individuals. The DAF 5′-regulatory sequence was verified in all individuals using cycle sequencing as described above. The EBV-transformed lymphoblasts were maintained in DMEM supplemented with 10% FBS and 1% P/S and checked for mycoplasma infection by Hoechst staining. For LPS (Sigma-Aldrich, Saint Louis, MO, USA) stimulation, cells were treated, as previously described, with 10 μg ml^{-1} LPS for 6 h[52] before harvesting for mRNA.

Plasmid constructs

The WT *DAF* promoter construct cloned into a pGL3-basic firefly luciferase reporter vector was gifted by Dr DuBois.[53] The Mut construct was generated by site-directed mutagenesis using the QuickChange kit (Stratagene, La Jolla, CA, USA) to mutate the C at c.-198 to G using the WT *DAF* promoter construct as a template. The mutant sequence was verified using an ABI Prism 3100 automated sequencer before further evaluation. The pRL-TK vector (Promega, Madison, WI, USA) was used as an internal control reporter to test for transfection efficiency. The pCMV-Sp1 expression vector was obtained from Dr Tijan (Department of Molecular and Cell Biology, University of California, Berkeley, CA, USA) through Addgene.

Transfections and reporter assays

Cells were plated at 1.5×10^5 cells per ml in six-well plates 1 day before transfection. Non-liposomal gene transfer was carried out using FuGENE 6 (Roche, Basel, Switzerland) according to the manufacturer's instructions with 1 μg of DNA consisting of the WT or the Mut *DAF* reporter construct, and/or Sp1 expression vector and the internal control vector. At 48 h after transfection, cells were analyzed for luciferase activity using the Dual-Luciferase Reporter Assay (Promega) following the manufacturer's instructions and quantified using a Luminoskan Ascent luminometer (Thermo LabSystems, Franklin, MA, USA). All transfections were carried out in duplicate.

TFBS analysis

We performed a direct matching of the known TFBSs contained in the TRANSFAC Professional database (v.11.2).[54] This was carried out using the Patch program of the TRANSFAC Suite.[54] We matched the motifs with a length of 7 bp, with no mismatch between the template motif and the matched sequence. We considered that the motif is affected by the SNP if it includes the SNP nucleotide. Our results indicate that an Sp1-binding site in genomic sequence (C nucleotide version) is lost when G nucleotide replaced C nucleotide. The new putative TFBS obtained was that of a NF-κB-binding site.

Western blot

Whole-cell extracts were prepared from cells using a lysis buffer containing: 150 mM NaCl, 1% Triton X-100, 50 mM Tris-HCl (pH 8.0), supplemented with 1 mg ml^{-1} of aprotinin, 1 mg ml^{-1} of Pepstatin A and 2 mM of phenylmethanesulfonyl fluoride protease inhibitors (Sigma-Aldrich). Proteins were resolved on 8% SDS–polyacrylamide gels under non-reducing conditions and transferred to Hybond ECL (Amersham Biosciences, Piscataway, NJ, USA). The membranes were probed with appropriate primary antibodies and detected using peroxidase-conjugated anti-mouse or anti-rabbit antibodies (1:5000) and visualized by enhanced chemiluminescence (Pierce, Rockford, IL, USA). The primary antibodies used were mouse monoclonal anti-DAF (1:100; BRIC 216, IBGRL, London, UK) and anti-p38 (1:5000; Cell Signaling Technology Inc., Beverly, MA, USA).

Statistical analysis

Allele and genotype frequencies were compared between groups using 2×2 tables to obtain a Yates corrected χ^2; if a cell value was <5 the Fisher exact test was used (http://www.openepi.com). Odds ratios and their 95% confidence intervals (CIs) were determined relative to control populations. The remaining calculations were carried out with Statistica 8.0 software (StatSoft Inc, Tulsa, OK, USA). Skewed data are represented by median and IQR. The differences in the time of evaluation between the racial groups were assessed using the Kruskal–Wallis test. $P<0.05$ (two-tailed) was considered statistically significant.

Conflict of interest

The authors declare no conflict of interest.

Acknowledgements

We thank Dr Ray du Bois (Vanderbilt University Medical Center) for his kind gift of the DNA construct of the human *DAF* promoter cloned upstream of a luciferase reporter gene, Dr Ed Ojuka (University of Cape Town (UCT) Sports Science) for the C2C12 muscle cell line, Ms Ingrid Baumgaarten (Chemical Pathology, UCT) for supervising the EBV lymphoblastoid cell line preparation, Dr Huajian Teng (Human Biology, UCT) for site-directed mutagenesis and Dr Motassim Badri (Medicine, UCT) for supervising statistical manipulations. This work was supported by a grant from the Muscular Dystrophy Association of South Africa (to JMH), University of Cape Town research grants (to SP and JMH), National Bioinformatics Network grants (to VBB) and National Research Foundation grants [61070 to VBB, 62302 to VBB and 64751 to VBB and MK]. HU was supported by the International Brian Research Organization's Levi Montalcini Fellowship and MK by the postdoctoral fellowship from the Claude Leon Foundation (South Africa).

References

1 Engel AG, Lambert EH, Howard FM. Immune complexes (IgG and C3) at the motor end-plate in myasthenia gravis. Ultrastructural and light microscopic localization and electrophysiological correlations. *Mayo Clin Proc* 1977; **52**: 267–280.
2 Lin F, Kaminski HJ, Conti-Fine BM, Wang W, Richmonds C, Medof ME. Markedly enhanced susceptibility to experimental autoimmune myasthenia gravis in the absence of

decay-accelerating factor protection. *J Clin Invest* 2002; **110**: 1269–1274.
3 Shahashi K, Engel AG, Lambert EH, Howard FM. Ultrastructural localization of the terminal and lytic ninth complement component (C9) at the motor end-plate in myasthenia gravis. *J Neuropath Exp Neurol* 1980; **39**: 160–172.
4 Drachman DB, Angus CW, Adams RN, Michelson JD, Hoffman GJ. Myasthenic antibodies cross-link acetylcholine receptors to accelerate degradation. *N Engl J Med* 1978; **298**: 1116–1122.
5 Sahashi K, Engel AG, Lindstrom JM, Lambert EH, Lennon VA. Ultrastructural localization of immune complexes (IgG and C3) at the end-plate in experimental autoimmune myasthenia gravis. *J Neuropathol Exp Neurol* 1978; **37**: 212–223.
6 Lennon VA, Seybold ME, Lindstrom J, Cochrane C, Ulevitch R. Role of complement in the pathogenesis of experimental autoimmune myasthenia gravis. *J Exp Med* 1978; **147**: 973–983.
7 Biescker G, Gomez CM. Inhibition of acute passive transfer experimental autoimmune myasthenia gravis with Fab antibody to complement C5. *Immunology* 1989; **142**: 2654–2659.
8 Piddlesden SJ, Jiang S, Levin JL, Vincent A, Morgan BP. Soluble complement receptor 1 (sCR1) protects against experimental autoimmune myasthenia gravis. *J Neuroimmunol* 1996; **71**: 173–177.
9 Chamberlain-Banoub J, Neal JW, Mizuno M, Harris CL, Morgan BP. Complement membrane attack is required for end-plate damage and clinical disease in passive experimental myasthenia gravis in Lewis rats. *Clin Exp Immunol* 2006; **146**: 278–286.
10 Tüzün E, Scott BG, Goloszko E, Higgs S, Christadoss P. Genetic evidence for involvement of classical complement pathway in induction of experimental autoimmune myasthenia gravis. *J Immunol* 2003; **171**: 3847–3854.
11 Ruff RL, Lennon VA. How myasthenia alters the safety factor for neuromuscular transmission. *J Neuroimmunol* 2008; **201–202**: 13–20.
12 Medof ME, Kinoshita T, Nussenzweig V. Inhibition of complement activation on the surface of cells after incorporation of decay accelerating factor (DAF) into their membranes. *J Exp Med* 1984; **160**: 1558–1578.
13 Fujita T, Inoue T, Ogawa K, Iida K, Tamura N. The mechanism of action of decay-accelerating factor (DAF). DAF inhibits the assembly of C3 convertases by dissociating C2a and Bb. *J Exp Med* 1987; **166**: 1221–1228.
14 Kaminski HJ, Li Z, Richmonds C, Lin F, Medof ME. Complement regulators in extraocular muscle and experimental autoimmune myasthenia gravis. *Exp Neurol* 2004; **189**: 333–342.
15 Kaminski HJ, Kusner LL, Richmonds C, Medof ME, Lin F. Deficiency of decay accelerating factor and CD59 leads to crisis in experimental myasthenia. *Exp Neurol* 2006; **202**: 287–293.
16 Morgan BP, Chamberlain-Banoub J, Neal JW, Song W, Mizuno M, Harris CL. The membrane attack pathway of complement drives pathology in passively induced experimental autoimmune myasthenia gravis in mice. *Clin Exp Immunol* 2006; **146**: 294–302.
17 Heckmann JM, Owen EP, Little F. Myasthenia gravis in South Africans: racial differences in clinical manifestations. *Neuromuscul Disord* 2007; **17**: 929–934.
18 Lass JH, Walter EI, Burris TE, Grossniklaus HE, Roat MI, Skelnik DL *et al*. Expression of two molecular forms of the complement decay-accelerating factor in the eye and lacrimal gland. *Invest Ophthalmol Vis Sci* 1990; **31**: 1136–1148.
19 Porter JD, Khanna S, Kaminski HJ, Rao JS, Merriam AP, Richmonds CR *et al*. Extraocular muscle is defined by a fundamentally distinct gene expression profile. *Proc Natl Acad Sci USA* 2001; **98**: 12062–12067.
20 Post TW, Arce MA, Liszewski MK, Thompson ES, Atkinson JP, Lublin DM. Structure of the gene for human complement protein decay accelerating factor. *J Immunol* 1990; **144**: 740–744.
21 Osuka F, Endo Y, Higuchi M, Suzuki H, Shio Y, Fujiu K *et al*. Molecular cloning and characterization of novel splicing variants of human decay-accelerating factor. *Genomics* 2006; **88**: 316–322.
22 Coyne KE, Hall SE, Thompson ES, Arce MA, Kinoshita T, Fuijita T *et al*. Mapping epitopes, glycosylation sites, and complement regulatory domains in human decay accelerating factor. *J Immunol* 1992; **149**: 2906–2913.
23 Brodbeck WG, Kuttner-Kondo L, Mold C, Medof ME. Structure/function studies of human decay-accelerating factor. *Immunology* 2000; **101**: 104–111.
24 Caras IW, Davitz MA, Rhee L, Davitz MA, Rhee L, Weddell G *et al*. Cloning of decay accelerating factor suggests novel use of splicing to generate two proteins. *Nature* 1987; **325**: 545–548.
25 Moran P, Raab H, Kohr WJ, Caras IW. Glycophospholipid membrane anchor attachment. Molecular analysis of the cleavage/attachment site. *J Biol Chem* 1991; **266**: 1250–1257.
26 Ewulonu UK, Ravi L, Medof ME. Characterization of the decay-accelerating factor gene promoter region. *Proc Natl Acad Sci USA* 1991; **88**: 4675–4679.
27 Thomas DJ, Lublin DM. Identification of 5′-flanking regions affecting the expression of the human decay accelerating factor gene and their role in tissue-specific expression. *J Immunol* 1993; **150**: 151–160.
28 Cauvi DM, Cauvi G, Pollard KM. Constitutive expression of murine decay-accelerating factor 1 is controlled by the transcription factor Sp1. *J Immunol* 2006; **177**: 3837–3847.
29 Knight JC. Regulatory polymorphisms underlying complex disease traits. *J Mol Med* 2005; **83**: 97–109.
30 Soltys J, Gong B, Kaminski HJ, Zhou Y, Kusner LL. Extraocular muscle susceptibility to myasthenia gravis. Unique immunological environment? *Ann N Y Acad Sci* 2008; **1132**: 220–224.
31 Brivanlou AH, Darnell Jr JE. Signal transduction and the control of gene expression. *Science* 2002; **295**: 813–818.
32 Courey AJ, Holtzman DA, Jackson SP, Tijan R. Synergistic activation by the glutamine-rich domains of human transcription factor Sp1. *Cell* 1989; **59**: 827–836.
33 Boisclair YR, Brown AL, Casola S, Rechler MM. Three clustered Sp1 sites are required for efficient transcription of the TATA-less promoter of the gene for insulin-like growth factor-binding protein-2 from the rat. *J Biol Chem* 1993; **268**: 24892–24901.
34 Dusing MR, Wiginton DA. Sp1 is essential for both enhancer-mediated and basal activation of the TATA-less human adenosine deaminase promoter. *Nucleic Acids Res* 1994; **22**: 669–677.
35 Pastinen T, Slavek R, Gurd S, Sammak A, Ge B, Lepage P *et al*. A survey of genetic and epigenetic variation affecting human gene expression. *Physiol Genomics* 2003; **16**: 184–193.
36 Udalvo IA, Richardson A, Denys A, Smith C, Ackerman H, Foxwell B *et al*. Functional consequences of a polymorphism affecting NF-κB p50–p50 binding to the *TNF* promoter region. *Mol Cell Biol* 2000; **20**: 9113–9119.
37 Liu J, Miwa T, Hilliard B, Chen Y, Lambris JD, Wells AD *et al*. The complement inhibitory protein DAF (CD55) suppresses T cell immunity *in vivo*. *J Exp Med* 2005; **201**: 567–577.
38 Heeger PS, Lalli PN, Lin F, Valujskikh A, Lui J, Muqim N *et al*. Decay-accelerating factor modulates induction of T cell immunity. *J Exp Med* 2005; **201**: 1523–1530.
39 Soltys J, Kusner L, Young A, Richmonds C, Hatala D, Gong B *et al*. Novel complement inhibitor limits severity of experimental myasthenia gravis. *Ann Neurol* 2009; **65**: 67–75.
40 Nicholson-Weller A, March JP, Rosenfeld SI, Austen KF. Affected erythrocytes of patients with paroxysmal nocturnal hemoglobinuria are deficient in the complement regulatory protein, decay accelerating factor. *Proc Natl Acad Sci USA* 1983; **80**: 5066–5070.
41 Pangburn MK, Schreiber RD, Muller-Eberhard HJ. Deficiency of an erythrocyte membrane protein with complement regulatory activity in paroxysmal nocturnal hemoglobinuria. *Proc Natl Acad Sci USA* 1983; **80**: 5430–5434.

42 Lublin DM, Mallinson G, Poole J, Reid ME, Thompson ES, Ferdman BR *et al*. Molecular basis of reduced or absent expression of decay-accelerating factor in Cromer blood group phenotypes. *Blood* 1994; **84**: 1276–1282.
43 Taniguchi H, Lowe CE, Cooper JD, Smyth D, Bailey R *et al*. Discovery, linkage disequilibrium and association analyses of polymorphisms of the immune complement inhibitor, decay-accelerating factor gene (DAF/CD55) in type I diabetes. *BMC Genetics* 2006; **7**: 22–31.
44 Christmas SE, de la Mata Espinosa CT, Halliday D, Buxton CA, Cummerson A, Johnson PM. Levels of expression of complement regulatory proteins CD46, CD55 and CD59 on resting and activated human peripheral blood leucocytes. *Immunology* 2006; **119**: 522–528.
45 Miwa T, Maldonado MA, Zhou L, Yamada K, Gilkeson GS, Eisenberg RA *et al*. Decay-accelerating factor ameliorates systemic autoimmune disease in MRL/lpr mice via both complement-dependent and -independent mechanisms. *Am J Path* 2007; **170**: 1258–1266.
46 Zhou Y, Gong B, Lin F, Rother RP, Medof ME, Kaminski HJ. Anti-C5 antibody treatment ameliorates weakness in experimentally acquired myasthenia gravis. *J Immunol* 2007; **179**: 8562–8567.
47 Hillmen P, Young NS, Schubert J, Brodsky RA, Socié G, Muus P *et al*. The complement inhibitor eculizumab in paroxysmal nocturnal hemoglobinuria. *N Engl J Med* 2006; **355**: 1233–1243.
48 Basta M, Van Goor F, Luccioli S, Billings EM, Vortmeyer AO, Baranyi L *et al*. F(ab)′$_2$-mediated neutralization of C3a and C5a anaphylatoxins: a novel effector function of immunoglobulins. *Nat Med* 2003; **9**: 431–438.
49 Livak KJ, Schittgen TD. Analysis of relative gene expression data using real-time quantitative PCR and the $2^{-\Delta\Delta CT}$ method. *Methods* 2001; **25**: 402–408.
50 Wong ML, Medrano JF. Real-time PCR for mRNA quantification. *Biotechniques* 2005; **39**: 75–85.
51 Nolan T, Hands RE, Bustin SA. Quantification of mRNA using real-time RT-PCR. *Nat Protoc* 2006; **1**: 1559–1582.
52 Iborra A, Mayorga M, Llobet N, Martinez P. Expression of complement regulatory proteins [membrane cofactor protein (CD46), decay accelerating factor (CD55), and protectin (CD59)] in endometrial stressed cells. *Cell Immunol* 2003; **223**: 46–51.
53 Holla VR, Wang D, Brown JR, Mann JR, Katkuri S, DuBois RN. Prostaglandin E_2 regulates the complement inhibitor CD55/decay-accelerating factor in colorectal cancer. *J Biol Chem* 2005; **280**: 476–483.
54 Matys V, Kel-Margoulis OV, Fricke E, Liebich I, Land S, Barre-Dirrie A *et al*. TRANSFAC and its module TRANSCompel: transcriptional gene regulation in eukaryotes. *Nucl Acids Res* 2006; **34**(Database issue): D108–D110.

This work is licensed under the Creative Commons Attribution-NonCommercial-No Derivative Works 3.0 Licence. To view a copy of this licence, visit http://creativecommons.org/licenses/by-nc-nd/3.0/

Supplementary Information accompanies the paper on Genes and Immunity website (http://www.nature.com/gene)